International Journal of Refractory Metals and Hard Materials 125 (2024) 106892



Contents lists available at ScienceDirect

International Journal of Refractory Metals and Hard Materials

journal homepage: www.elsevier.com/locate/IJRMHM





Field-assisted sintering of MC-Ti_3SiC_2 composites with adjustable thermal expansion coefficient

Leonhard Gertlowski [a,b,*], Simone Herzog [a], Sofia Fries [b], Christoph Broeckmann [a,b]

[a] Institute for Materials Applications in Mechanical Engineering (IWM), RWTH Aachen University, 52062 Aachen, Germany
[b] Institute of Applied Powder Metallurgy and Ceramics at RWTH Aachen e.V. (IAPK), 52062 Aachen, Germany

ARTICLE INFO

Keywords:
MAX phase Ti_3SiC_2
Field-assisted sintering
Carbide content
Coefficient of thermal expansion
Precision glass moulding

ABSTRACT

Tool materials for precision glass moulding made of WC or SiC bear the risk of glass breakage due to a difference in the coefficient of thermal expansion (CTE) between the mould and the glass. The aim of this study is to develop a MAX phase composite with increased CTE and thus reduced CTE difference. A mixture of Ti_3SiC_2 and 10 vol% SiC powder was sintered between 1250 °C and 1350 °C using the field-assisted sintering technique (FAST). In addition to the sintering temperature, the dwell time and the initial particle size were varied using a full factorial experimental design. Complete densification, homogeneous carbide distribution and no grain coarsening were observed for specimens sintered at 1300 °C for 10 min at 50 MPa. The grain size of SiC and Ti_3SiC_2 is approximately 0.3 µm, although larger grains occasionally occur. Identified process parameters were successfully transferred to TiC reinforced Ti_3SiC_2 composites. While the carbide content can be specifically controlled by mixing, the MAX phase partially decomposes during sintering. MC additions between 10 and 30 vol% resulted in an adjustable CTE in the range 6.8–9.0 ppm/K.

1. Introduction

MAX phases are a group of materials that cannot be clearly classified as either metals or ceramics and have an unusual combination of material properties [1]. High electrical and thermal conductivity, thermal shock resistance and excellent machinability as well as the tolerance to brittle failure characterise the metallic nature of the MAX phases [2,3]. On the other hand, they have a high specific stiffness, high strength at high temperatures and they are resistant to oxidation and corrosion [4–7]. These are typical properties of ceramics. MAX phases ($M_{n+1}AX_n$) are composed of three different elements. The element “M” is a transition metal from groups 3 to 6 of the periodic table. “A” is an element from groups 12 to 16 and “X” is either carbon and/or nitrogen. The atoms M, A and X can be partially substituted. n can take the value 1, 2 or 3. [8]

In this study, a composite with the 312-phase of the Si-Ti-C system as the matrix is investigated. Ti_3SiC_2 has a high CTE with a value of 9.1 · 10^{-6} K^{-1} [9]. The CTE is almost twice that of tungsten carbide [10]. Compared to the CTE of the MAX phase, the CTE of SiC is approximately 3.2–5.1 · 10^{-6} K^{-1} between room temperature (RT) and 1000 °C [11–15]. The CTE of TiC is 7.4–7.7 · 10^{-6} K^{-1} [12,16–18]. There are only a few studies that have investigated the effect of the carbide content on the CTE of the composite. The differences in the CTE between the phases are used to explain the loss of strength. According to Ho-Duc et al. [19] the CTE of a composite with a Ti_3SiC_2 matrix and 30 vol% carbides is 8.2 · 10^{-6} K^{-1}. This value is independent of whether SiC or TiC is used as the reinforcing phase.

The adjustability of the CTE makes MAX phase composites an interesting candidate for precision glass moulding. This glass moulding process is used to produce glass lenses with complex geometries and high repeatability [20,21]. Stresses in the glass are caused by a CTE difference between the glass and the mould [22]. In order to avoid stresses and possible glass breakage, the aim is to achieve the smallest possible CTE difference between the glass and the mould. Tungsten carbide with a CTE of 4.9 · 10^{-6} K^{-1} is conventionally used as the mould material [20,23]. It differs from optical glass in terms of CTE [20]. Soda-lime glass, which is used as a glass material in precision glass moulding due to its low transition temperature, has a CTE of 7.2 · 10^{-6} K^{-1} between 100 °C und 300 °C [24].

Ti_3SiC_2 has been synthesized in numerous scientific papers. The studies differ in the use of starting powders, stoichiometry, sintering technique and sintering parameters. Most studies used the powder

* Corresponding author at: Institute for Materials Applications in Mechanical Engineering (IWM), RWTH Aachen University, 52062 Aachen, Germany.
E-mail address: l.gertlowski@iwm.rwth-aachen.de (L. Gertlowski).

https://doi.org/10.1016/j.ijrmhm.2024.106892
Received 17 April 2024; Received in revised form 22 July 2024; Accepted 14 September 2024
Available online 16 September 2024
0263-4368/© 2024 The Authors. Published by Elsevier Ltd. This is an open access article under the CC BY license (http://creativecommons.org/licenses/by/4.0/).

mixtures Ti/Si/C [25–32], Ti/TiC/Si [31,33–35] or Ti/SiC/C [31,36–39]. The synthesis of multiphase materials with Ti_3SiC_2 matrix is part of several research works. Barsoum and El-Raghy [7] already recognised the potential of Ti_3SiC_2 composites. SiC and TiC are usually used as reinforcing phases due to their thermodynamic stability [2,3]. Two different sintering routes exist for the synthesis of SiC/TiC-Ti_3SiC_2 composites. On the one hand, the composites can be produced by sintering of pre-alloyed powders [33]. On the other hand, the composites can be synthesized by reaction sintering [3,19,40–44]. According to Tian et al. [43] the optimum sintering temperature for the synthesis of completely densified composites is 1400 °C for field-assisted reaction sintering, which is higher than for the synthesis without a reinforcing phase. However, at higher sintering temperatures, the MAX phase starts to decompose again [25,45]. This is the result of the narrow stable region of Ti_3SiC_2 in the ternary phase diagram of Titanium, Silicon and Carbide [46]. The formation of $TiSi_2$ and Ti_5Si_3 is sometimes observed [27,29,47,48]. The literature is divided on possible reaction products.

In this study a mixture of Ti_3SiC_2 and 10 vol% SiC powder is sintered between 1250 °C and 1350 °C for different dwell times using the field-assisted sintering technique. The purpose of this work is to investigate the consolidation of the MAX phase composites as a function of process parameters and particle size in order to develop a fully densified and fine-grained material with a homogeneous carbide distribution as a moulding material for precision glass moulding. The consolidation of the composites is evaluated on the basis of porosity and grain size, selecting the process parameters that produce the finest-grained microstructure at full densification to meet the requirements of the ultra-precision machining used to produce the mould shape. Larger crystallographic grains and porosity lead to brittle machining during ultra-precision machining. The imperfections of the mould surface due to brittle machining are imprinted on the glass lens to be produced and reduce the quality of the optical application. Furthermore, the manufacturing process consisting of grinding, mixing and sintering is to be evaluated based on possible tertiary phases and impurities. The aim is to find out whether $TiSi_2$ and Ti_5Si_3 are formed during the field-assisted sintering technique and what influence they have on the thermophysical properties. Finally, following the development of a fully densified and fine-grained MAX phase composite suitable for ultra-precision machining in order to produce the mould shape, the thermophysical properties of the composites are described as the content of the reinforcing phase is varied. The CTE of the MAX phase composites is adjusted by the carbide content. To reduce the CTE difference between the moulding material and different glasses with different CTEs, a mixing rule is developed to produce a customised MAX phase composite for each glass.

2. Materials and methods

In this study, a mixture of pre-alloyed Ti_3SiC_2 powder with 10 vol% carbide powder is used. In the first step, only SiC is used. After identifying good process parameters, SiC is replaced by TiC as the reinforcing phase. The powders are ground separately before sintering. A *Pulverisette 5 (Fritsch)* planetary ball mill rotating at 250 rpm is used for the grinding process. The grinding jars and balls are made of tungsten carbide. The grinding balls have a diameter of 20 mm. The grinding jars have a volume of 250 cm^3. A ball to powder weight ratio of approximately 8:1 is used. The powders are wet milled using isopropanol, producing two fractions by varying the grinding time. The first fraction of each powder is milled for 2 h and the second fraction for 4 h. After grinding, the powders are dried separately for 12 h at 85 °C.

In this investigation, powder blends are only made by mixing Ti_3SiC_2 and SiC (respectively TiC) powders ground for the same time. 90 vol% Ti_3SiC_2 is mixed with 10 vol% SiC (respectively TiC). In the following, mixtures, consisting of powders that have been ground for 2 h, are referred to as *coarse (c)*, while the other mixtures are referred to as *fine (f)*. A tumbling mixer is used to homogenise the powder mixtures. The particle size and specific surface area of the different powders are given in Table 1. It should be noted that the powder particles tend to agglomerate.

After grinding and blending the powders, the mixtures are sintered using the field-assisted sintering technique. The specimens are produced in a graphite die using a current that passed through the powder. Due to the high electrical conductivity of the MAX phase the powder is heated up by direct resistance heating. Specimens with a cylindrical shape and a diameter of 20 mm and height of 5 mm are sintered. The powder is unidirectionally compacted at 50 MPa during the sintering cycle using two graphite stamps. The temperature is measured by a pyrometer inside one of the stamps and is automatically controlled by the current. In this investigation, the sintering temperature is varied between 1250 °C and 1350 °C, while the dwell time is varied between 5 min and 40 min. In the following, *C-SiC-1350/10* is used to describe a SiC reinforced specimen, which consists of *coarse* powder and is sintered by using a sintering temperature of 1350 °C and a dwell time of 10 min. The full factorial design of this study is shown in Table 2.

All 24 samples are cut up and prepared ceramographically using a number of different polishing levels. Afterwards the prepared interfaces are investigated using light microscopes and the electron backscatter diffraction (EBSD) of the Dual Beam *Helios Nanolab G3 CX (FEI)*. The fraction of the two phases and any tertiary phases, the porosity, and the grain sizes are measured. In addition, the homogeneity of the carbide distribution is described using the coefficient of variation V from Eq. (1).

$$V = \frac{\sqrt{\frac{1}{n}\cdot\sum_{i}^{n}(x_i-\overline{x})^2}}{\overline{x}}. \quad (1)$$

x_i is either the carbide fraction or the average size of the carbide particles in a square image section i of the light microscopy images with an edge length of 50 µm. The coefficient of variation is calculated from n = 160 image sections for each sample. $\overline{x}$ is the arithmetic mean of the measured size. Occasionally, the material structure is imaged using scanning transmission electron microscopy (STEM). This is done by cutting lamellae out of the microstructure with a gallium ion beam and thinning them successively. When the samples are less than 100 nm thick, they are analysed by STEM. The experiment is carried out in the *Dual Beam Helios Nanolab G3 CX (FEI)*. As mentioned in the introduction, the consolidation process is evaluated based on the porosity and grain size of the sintered MAX phase composite with a homogeneous carbide distribution. As the MAX phase composite is to be used as a mould for precision glass moulding, it has to be machined using ultra-precision machining to reproduce the desired shape of the optical component. Ultra-precision machining requires a fully compacted material. This means that there has to be no residual porosity. Full densification is an exclusion criterion. Among the fully densified composites, the one with the smallest grain size should be selected to meet the requirements of ductile machining for ultra-precision machining. The small grain size reduces the risk of brittle machining resulting in an inhomogeneous mould surface. Any imperfections will be reflected as defects in the glass lenses to be moulded, reducing the quality of the optical application. When several process parameters result in a fully densified MAX phase

Table 1
Particle size and specific surface area of the separated powders depending on the grinding time, determined using the *Mastersize 3000 (Malvern Panalytical)* laser diffraction analyser.

Powder	Grinding time [h]	Particle size D50 [µm]	Specific surface area [m^2/kg]
Ti_3SiC_2	0 (initial)	28.7	365
	2 (coarse)	7.59	1625
	4 (fine)	7.39	1800
SiC	0 (initial)	3.17	3984
	2 (coarse)	2.38	5248
	4 (fine)	2.30	5361

Table 2
Full factorial design of sintering SiC-Ti_3SiC_2 specimens.

					Number of variations
dwell time	5 min	10 min	20 min	40 min	4
sintering temperature	1250 °C	1300 °C	1350 °C	–	3
grinding time	2 h / coarse	4 h / fine	–	–	2
					∑24

composite with identical smallest grain size, the parameter combination with the lowest sintering temperature is selected to minimise the MAX phase decomposition as postulated in the literature. The shortest dwell time at the selected sintering temperature is then chosen. Once the optimum process parameters have been identified for MAX phase composites with 10 vol% SiC, the sintering parameters are transferred to TiC reinforced Ti_3SiC_2 composites. The carbide content is varied and the thermophysical properties are investigated. Samples are sintered consisting of 10 vol%, 20 vol% and 30 vol% SiC as well as specimens consisting of Ti_3SiC_2 and TiC. Specimens without a reinforcing phase are also produced as a reference. The thermal conductivity is calculated as the product of thermal diffusivity, specific heat capacity and density. The thermal diffusivity is measured using the laser flash apparatus *LFA 427 (Netzsch)*. The mean value of 8 laser pulses is calculated for each temperature level. The discrete temperature levels are RT and the temperatures that satisfy the equation $\{100\,°C + x \cdot 100\,°C \mid 0 \leq x \leq 7\}$. The differential scanning calorimetry (DSC) is used to determine the heat capacity for the temperature interval [RT; 800 °C]. Measurements are made with the *DSC 404C (Netzsch)* in accordance with DIN 51007. Thermal diffusivity and heat capacity are measured in an argon atmosphere. Density is determined at RT according to the Archimedean principle and is calculated for different temperature levels using the thermal expansion results. In addition to the thermal conductivity measurements, the CTE of the composites is measured between RT and 800 °C under an argon flow. This thermophysical property is measured using the dilatometer *DIL 402C/4/G (Netzsch)*. The heating rate is 10 K/min.

3. Results and discussion

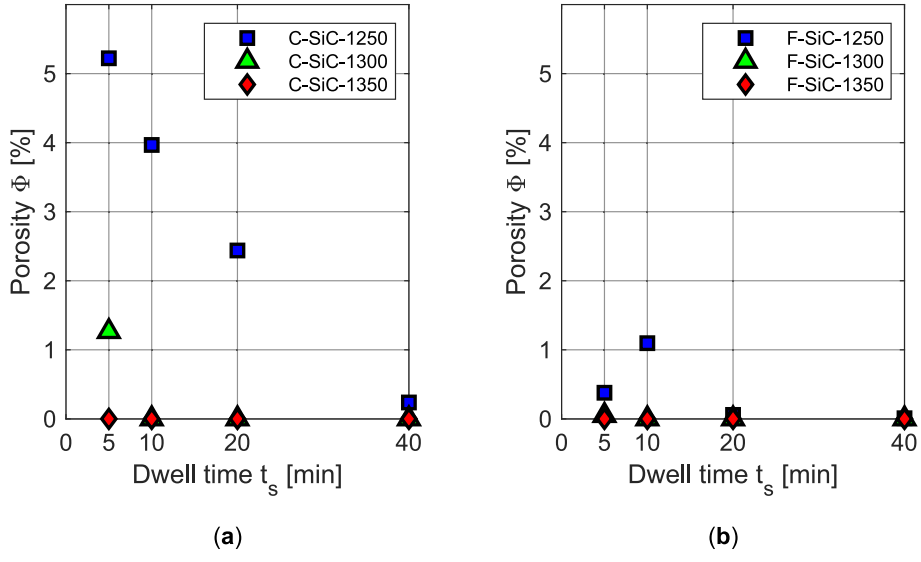
3.1. Densification

Abrasion during the grinding process results in tungsten carbide contamination of the powders, as the grinding jars and balls are made of tungsten carbide. For the use of MAX phase composites as moulds in precision glass moulding, the slight contamination with tungsten carbide, which is less than 2 vol%, is not considered critical. On the one hand, the moulding tools are conventionally made of tungsten carbide and, on the other hand, tungsten carbide can be regarded as a neutral addition to the reinforcing phase silicon carbide with a similar CTE. However, contamination by tungsten carbide makes it difficult to evaluate densification using density measurements based on the Archimedean principle or a gas pycnometer, as tungsten carbide increases the density of the samples. Porosity was therefore determined using light microscopy images. The results of the porosity measurement are shown in Fig. 1.

Firstly, it should be noted that the fine powder samples compact faster than the coarse powder samples. This observation is consistent with the idea that the sintering process is controlled by diffusion. The reduction in surface energy is a driving force for sintering. Since the specific surface area of the fine MAX phase powder is significantly larger than that of the coarse MAX phase powder according to Table 1, accelerated sintering kinetics are assumed. Regardless of the particle size, complete densification occurs when the samples are sintered at a minimum of 1300 °C for at least 10 min or at 1350 °C for 5 min. In contrast to Tian et al. [43], the samples are already densified at 1300 °C. An enlarged section of Fig. 1(b) is shown in Fig. 2. It shows that residual porosity remains at the lowest sintering temperature.

3.2. Phases

As briefly mentioned above, three phases and a small amount of tungsten carbide can be detected using the EBSD technique. In addition to Ti_3SiC_2 and SiC, $TiSi_2$ could be measured. SiC could also be detected from the light microscopy images by using a suitable contrast. The SiC content measured in the microscopic images corresponds approximately to the added 10 vol% SiC. This means that the carbide content of the composite can be specifically controlled by adding SiC to Ti_3SiC_2 powder. The content of Ti_3SiC_2 and in particular the tertiary phase $TiSi_2$ can only be determined with a measurement accuracy. This results from the fact that the electron beam stimulates several grains during the EBSD



(a) (b)

Fig. 1. Porosity measurements as a function of dwell time and sintering temperature for samples made from (a) coarse powder and (b) fine powder.

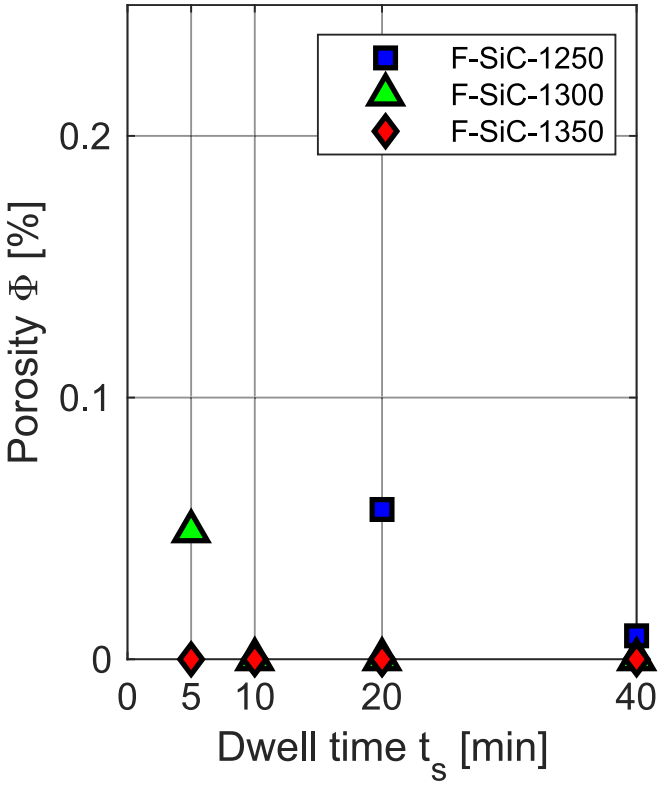


Fig. 2. Enlarged section of Fig. 1(b), showing the porosity measurements as a function of dwell time and sintering temperature for samples made from fine powder.

measurement due to the fine microstructure. The pattern of backscattered electrons is a superposition of different orientations or even phases. This makes it difficult to classify the phases. A phase-indexing of the three phases Ti_3SiC_2, SiC and $TiSi_2$ is shown in Fig. 3. With a step size of 80 nm, a square area of 80 µm × 80 µm was scanned. Black pixels do not indicate porosity, but areas where indexing was not possible.

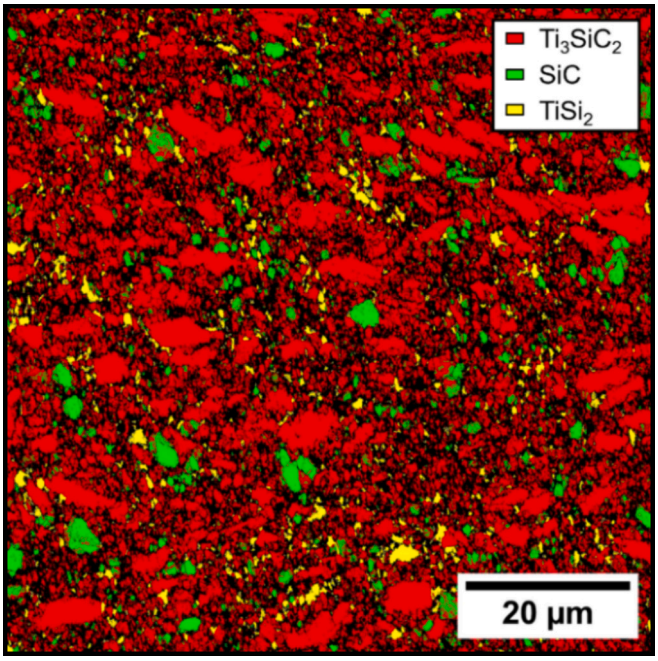


Fig. 3. EBSD phase-indexing of the specimen F-SiC-1250/40.

3.3. Grain growth and carbide distribution

No grain growth of the three phases was observed during the study. In particular, Fig. 4 shows that the size of the crystallographic grains of the MAX phase is approximately constant over time. The specimens sintered at 1250 °C and made from coarse powder deviate slightly from this.

This observation contradicts the expectation of grain coarsening. It is well known that the total energy of a sintering system tends towards an energy minimum. The reduction of the total energy, which includes surface and interfacial energy, forms the driving force of sintering. Grain boundaries are interfaces of the sintering system. The reduction of the interfacial energy is the cause of grain growth [49].

Based on the driving force of the sintering system, grain growth would be expected. The fact that no grain growth was observed suggests that the carbides act as grain growth inhibitors. This hypothesis is consistent with some studies describing the reduced grain boundary mobility of the MAX phase due to carbides [3,19,42]. In addition, grain growth is probably further reduced by the formation of the tertiary phase between the MAX phase grains. It is assumed that the tertiary phase also acts as a grain growth inhibitor. Furthermore, the rapid heating rate at the start of the FAST cycle and the relatively low sintering temperature reduce the grain growth.

Moreover, the very fine microstructure should also be highlighted. The crystallographic grains are very small. The grain size of the MAX phase and of SiC is about 0.3 µm. The grain size of the tertiary phase $TiSi_2$ is even slightly smaller. However, larger crystallographic grains of the MAX phase are occasionally visible. To avoid the sporadic larger grains, reaction sintering with elemental base powders should be considered.

An ultrathin lamella of the F-SiC-1300/10 sample is used to better resolve the microstructure of MAX phase composites. The lamella and the region of interest (ROI) are shown in Fig. 5. The lamella was cut with a gallium ion beam. A platinum layer was deposited on the sample to protect the lamella during the thinning process. The thickness of the lamella is less than 100 nm. It is fixed on a copper grid.

The fine microstructure of the MAX phase composites is shown in Fig. 6. All three images show the ROI from Fig. 5. Consistent with the values in Fig. 4, the crystallographic grains in Fig. 6 are very small. Grains smaller than 0.2 µm can be seen in Fig. 6(c). In addition to Ti_3SiC_2 and SiC the tertiary phase can also be detected. As mentioned in Fig. 3, the black pixels in Fig. 6(b) and (c) do not indicate porosity, but areas where indexing was not possible. It is suggested that the grains in these areas are too small for the EBSD technique. Multiple grains are stimulated by the electron beam. The superposition of the backscattered electrons cannot be analysed. This assumption is supported by the fact that the image quality appears to be sufficiently good as shown in Fig. 6 (a).

Carbides must be homogeneous and finely dispersed in the microstructure to effectively suppress grain growth. The carbide distribution is shown as an example in Fig. 7. It is evident that the SiC particles are homogeneously distributed. This supports the hypothesis that the carbides reduce the grain growth of the MAX phase. However, it should be noted that the carbide distribution alone cannot explain the crystallographic grains of Ti_3SiC_2 of 0.3 µm.

The carbide distribution was described by the coefficient of variation in Eq. (1). This method has rarely been used for description of the microstructure in the literature. The coefficient of variation is the same for almost all of the samples when the local carbide content is used as the test criterion. This indicates that the carbide distribution differs only slightly between the samples. This seems plausible. The powder preparation is identical and only the sintering parameters vary.

In particular, structural inhomogeneities are successfully indicated by a higher coefficient of variation. The coefficient of variation seems to be an excellent measure to quantitatively describe the carbide distribution.

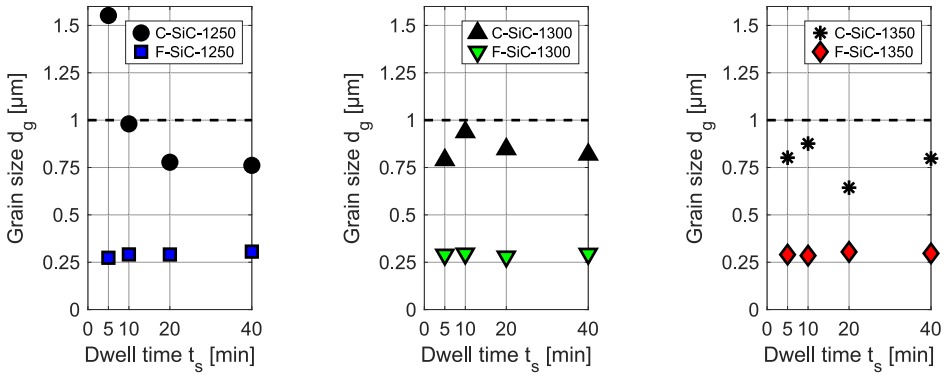


Fig. 4. Grain size of Ti_3SiC_2 grains depending on dwell time and particle size for the sintering temperatures (a) 1250 °C, (b) 1300 °C, and (c) 1350 °C.

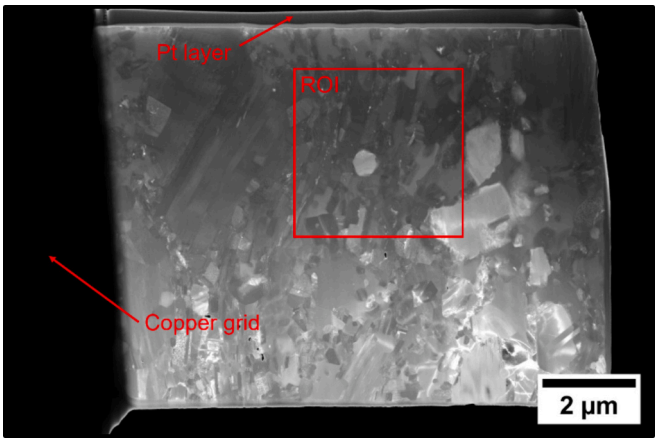


Fig. 5. Lamella of the specimen F-SiC-1300/10.

3.4. Sintering parameters

Sintering the SiC reinforced Ti_3SiC_2 composites at 1300 °C for 10 min using the fine powder best met the microstructural requirements. 1300 °C is the lowest sintering temperature with the shortest dwell time at which the samples are fully densified and the smallest grain size is present. The carbide content can be specifically adjusted by mixing and the carbides are homogeneously distributed. The MAX-phase composites, which are produced under the above-mentioned process parameters, are ideally suited to being manufactured to the shape of the glass lenses to be produced using ultra-precision machining.

The sintering parameters identified as optimal can be transferred to TiC reinforced Ti_3SiC_2 composites. The composites consisting of Ti_3SiC_2 and TiC are also fully densified and show a homogeneous microstructure. As an example of the fine microstructure, the image quality map (IQ) constructed from an EBSD measurement of a MAX phase composite containing 10 vol% TiC is shown in Fig. 8. The EBSD image was taken with a step width of 50 nm. Very small crystallographic grains can be seen in Fig. 8. The grains are significantly smaller than 1 µm. However, in addition to the small grains, some larger grains can also be seen.

The specimens produced to investigate the influence of the carbide content on the thermophysical properties in the following chapters are sintered at a sintering temperature of 1300 °C and a dwell time of 10 min. The finer powder is selected due to its smaller crystallographic grains. The slight increase in tungsten carbide contamination due to the longer grinding process is accepted. Chapter 3.1 has already discussed why the contamination is not critical.

3.5. Thermal expansion

The CTE is plotted against the temperature in Fig. 9. It varies with the type of carbide and its volume fraction in the composite. The CTE is between $6.6 \cdot 10^{-6}$ K^{-1} and $9.1 \cdot 10^{-6}$ K^{-1} in the temperature range [25 °C; 800 °C]. Above 200 °C the CTE increases approximately in proportion to the temperature. The CTE for the two temperature intervals [200 °C; 500 °C) and [500 °C; 800 °C] can be approximated as a linear function according to Eq. (2). m_1, m_2, CTE_{200} and CTE_{500} are

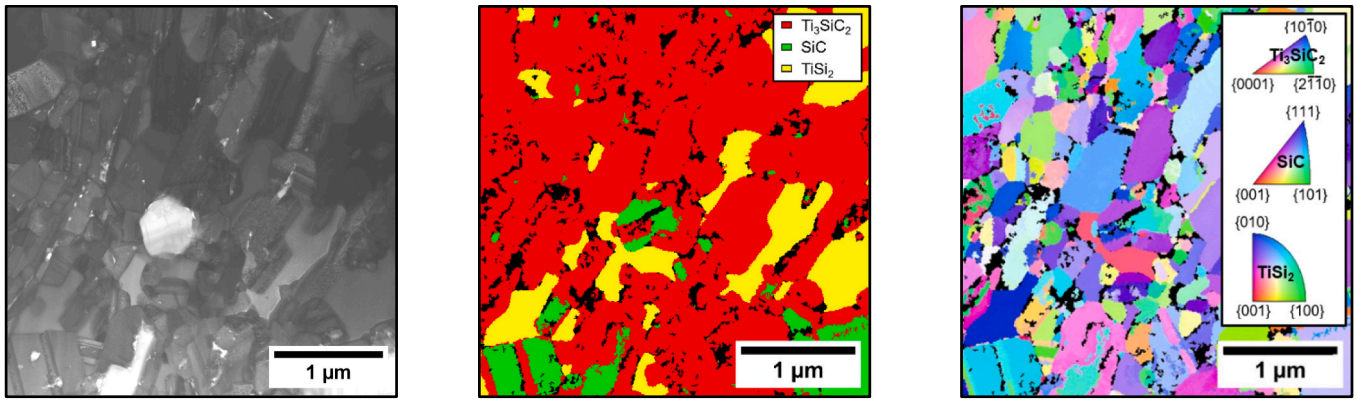


Fig. 6. Images of an ultrathin lamella of the specimen F-SiC-1300/10 using (a) STEM, (b) EBSD phase-indexing, and (c) EBSD inverse pole figure (IPF).

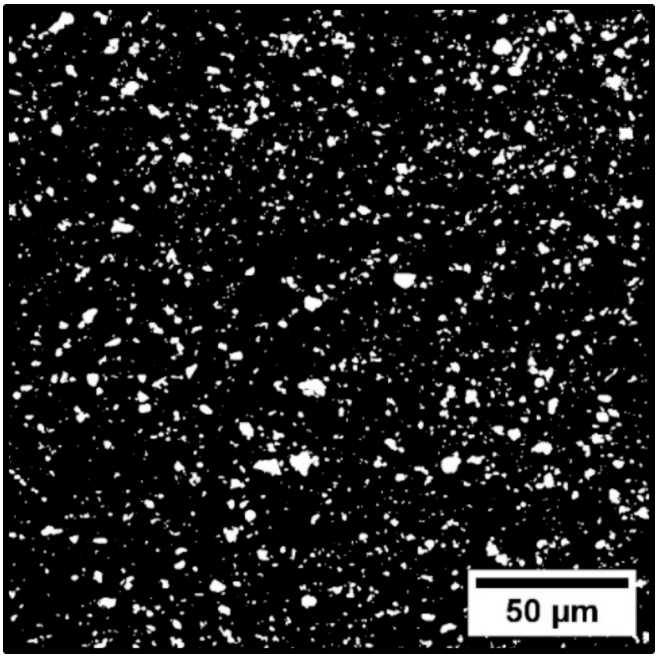


Fig. 7. Carbide distribution of the specimen F-SiC-1350/40. The white pixels are SiC.

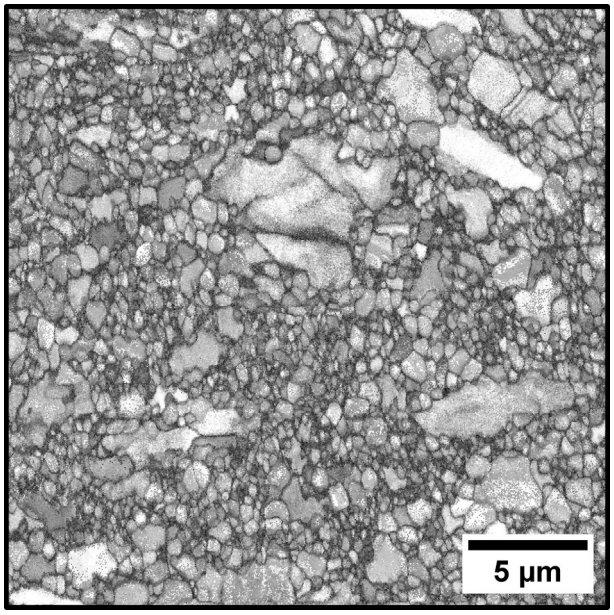


Fig. 8. IQ map of the specimen F-TiC-1300/10.

parameters for the linear approximation.

$$\mathrm{CTE}\,(T) = \begin{cases} \mathrm{m_1}\cdot(\mathrm{T} - 200^{\circ}\mathrm{C})\cdot\dfrac{\mathrm{K}}{^{\circ}\mathrm{C}} + \mathrm{CTE_{200}}\ \forall \mathrm{T} \in [200^{\circ}\mathrm{C}; 500^{\circ}\mathrm{C}) \\ \mathrm{m_2}\cdot(\mathrm{T} - 500^{\circ}\mathrm{C})\cdot\dfrac{\mathrm{K}}{^{\circ}\mathrm{C}} + \mathrm{CTE_{500}}\ \forall \mathrm{T} \in [500^{\circ}\mathrm{C}; 800^{\circ}\mathrm{C}] \end{cases} \quad (2)$$

Table 3 shows the parameters that have been found to approximate the coefficient of thermal expansion as a function of temperature. The values for the MAX phase composite consisting of 10 vol% SiC should be treated with caution as the graph in Fig. 9 deviates from a linear curve.

Using the approximation in Eq. 2 and the parameters in Table 3, it is possible to calculate the average CTE depending on the carbide content.

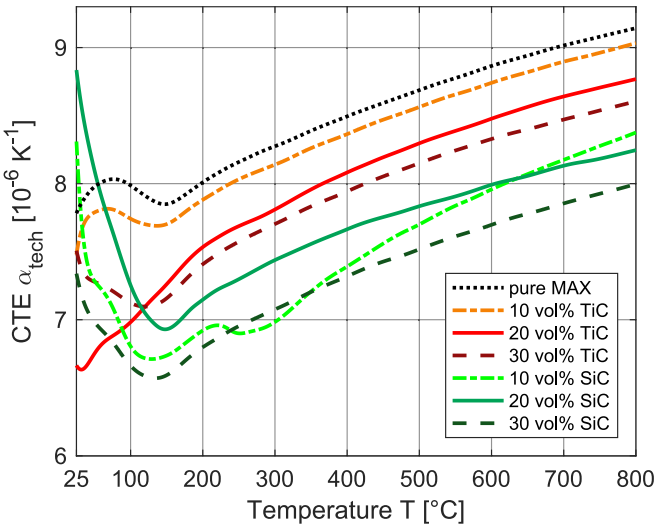


Fig. 9. CTE depending on temperature and carbide content.

Table 3
Parameters m_1 and m_2 in 10^{-9} K^{-2} and CTE_{200} and CTE_{500} in 10^{-6} K^{-1} to approximate CTE depending on the temperature.

	200–500 °C		500–800 °C	
	m_1	CTE_{200}	m_2	CTE_{500}
pure MAX	2.198	8.048	1.585	8.693
10 vol% TiC	2.220	7.916	1.544	8.581
20 vol% TiC	2.542	7.560	1.672	8.299
30 vol% TiC	2.416	7.453	1.480	8.171
10 vol% SiC	3.043	6.772	2.299	7.713
20 vol% SiC	2.265	7.196	1.484	7.827
30 vol% SiC	2.377	6.834	1.576	7.535

As mentioned above, the composites are three-phase materials consisting of Ti_3SiC_2, SiC/TiC and $TiSi_2$. However, in this study the average CTE is modelled using a two-phase mixing rule. This simplification seems plausible considering that the MAX phase and the tertiary phase with a CTE of $10.5 \cdot 10^{-6}$ K^{-1} between RT and 800 °C have almost identical coefficients of thermal expansion [50].

The average CTE is plotted against the carbide volume fraction in Fig. 10. It is obvious that the CTE is linearly dependent on the carbide content. The linear approximation is indicated by the dashed lines. It should be noted that the data points at 10 vol% SiC have been excluded.

The CTE of the composites can be successfully controlled by the

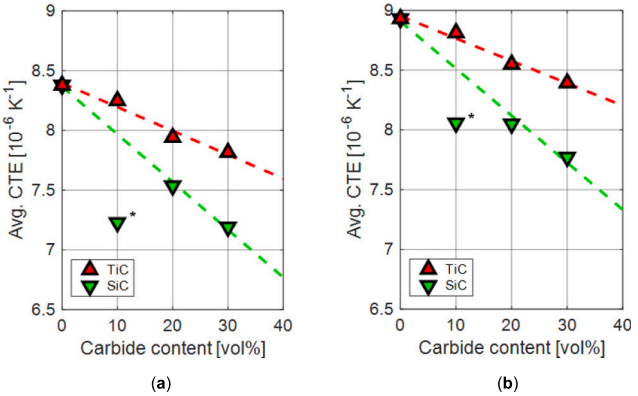


Fig. 10. Avg. CTE depending on carbide content for the temperature interval (a) 200 to 500 °C and (b) 500 to 800 °C. (* Data points not included in linear approximation).

carbide content. In addition, Fig. 10 confirms that SiC reduces the CTE of the composite more than TiC. This result seems to be plausible because TiC has a higher CTE than SiC. The linear approximation can be taken from Eq. (3) and Table 4. c is the carbide volume fraction of the composite. p and q are parameters for the linear approximation.

The CTE measurements support the hypothesis that MAX phase composites are suitable candidates for precision glass moulding. It is possible to use the carbide content to tailor the CTE of a moulding tool consisting of Ti_3SiC_2 and a reinforcing phase. The CTE difference between the glass and the mould could be reduced to protect glass lenses from glass breakage.

$$\text{avg.CTE}\ (c) = \text{p}\cdot\frac{c}{100\ \text{vol\%}} + \text{q}\cdot\left(1 - \frac{c}{100\ \text{vol\%}}\right) \quad (3)$$

3.6. Thermal conductivity

The thermal conductivity as the product of thermal diffusivity, heat capacity and density is plotted against the temperature in Fig. 11. The thermal conductivity was determined for discrete temperature values in the temperature interval [25 °C; 800 °C].

In general, two main findings can be noted: Firstly, the addition of the reinforcing phase leads to an increase in thermal conductivity. Secondly, the higher the carbide content of the composite, the higher the thermal conductivity. A higher thermal conductivity increases the suitability of a MAX phase composite for use as a moulding tool in precision glass moulding. A homogeneous temperature distribution is achieved more quickly [51]. It should also be noted that SiC reinforced composites have a higher thermal conductivity than TiC reinforced composites.

Finally, the effect of $TiSi_2$ formation on thermal conductivity should be evaluated. The formation of $TiSi_2$ is not a drawback for use as a moulding tool in precision glass moulding, as $TiSi_2$ has a comparatively high thermal conductivity of 52 W/(m·K) [52,53]. In fact, the formation of $TiSi_2$ has a positive effect on the cycle time of precision glass moulding.

4. Conclusions

The following results can be noted:

1. Field-assisted sintering at 1300 °C and 50 MPa for 10 min using a finely ground powder mixture consisting of Ti_3SiC_2 and SiC/TiC results in a completely densified composite.
2. The tertiary phase $TiSi_2$ is formed when pre-alloyed MAX phase powder is sintered using the field-assisted sintering technique.
3. No grain growth occurs during field-assisted sintering of SiC/TiC reinforced Ti_3SiC_2 composites.
4. The coefficient of variation seems to be an excellent measure to quantitatively describe the carbide distribution.
5. The CTE of the composites can be successfully controlled by the carbide content using a linear two-phase mixing rule.

Funding

This research was funded within the project “Mold materials with adjustable coefficient of thermal expansion for precision glass molding” by the German Research Foundation, grant number 506535305.

CRediT authorship contribution statement

Leonhard Gertlowski: Writing – original draft, Visualization, Software, Methodology, Investigation, Data curation, Conceptualization. **Simone Herzog:** Writing – review & editing, Supervision, Project administration, Methodology, Conceptualization. **Sofia Fries:** Writing – review & editing, Methodology, Funding acquisition. **Christoph Broeckmann:** Resources, Funding acquisition.

Table 4
Parameters in 10^{-6} K^{-1} to approximate avg. CTE depending on carbide volume fraction.

	200–500 °C		500–800 °C	
	p	q	p	q
SiC	4.374	8.367	4.966	8.908
TiC	6.400	8.395	7.077	8.953

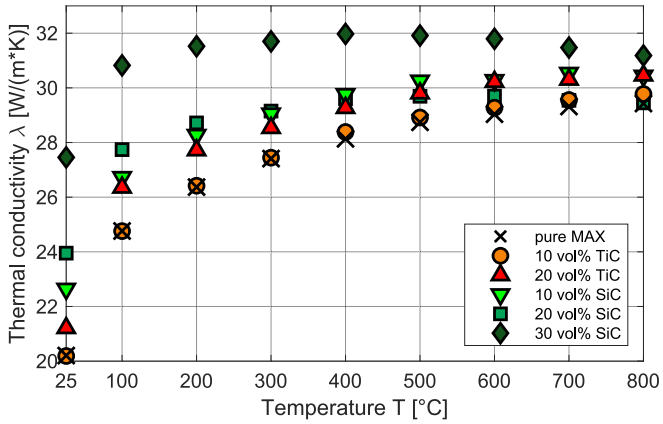


Fig. 11. Thermal conductivity depending on temperature and carbide content.

Declaration of competing interest

The authors declare no conflicts of interest.

Data availability

Data will be made available on request.

Acknowledgments

We acknowledge the funding from the German Research Foundation. We also acknowledge Malte Schmachtenberg’s SEM investigations and valuable discussions. Furthermore, we thank our project partners from the Manufacturing Technology Institute for their project cooperation.

References

[1] M. Radovic, M.W. Barsoum, MAX phases: bridging the gap between metals and ceramics, Am. Ceram. Soc. Bull. 92 (3) (2013) 20–27.
[2] Z.M. Sun, Progress in research and development on MAX phases: a family of layered ternary compounds, Int. Mater. Rev. 56 (3) (2011) 143–166, https://doi.org/10.1179/1743280410Y.0000000001.
[3] S.H. Amiri, M.G. Kakroudi, N.P. Vafa, M.S. Asl, Synthesis and sintering of Ti3SiC2–SiC composites through reactive hot-pressing of TiC and Si precursors, Silicon 14 (8) (2022) 4227–4235, https://doi.org/10.1007/s12633-021-01207-z.
[4] M.W. Barsoum, M. Radovic, Elastic and mechanical properties of the MAX phases, Annu. Rev. Mat. Res. 41 (1) (2011) 195–227, https://doi.org/10.1146/annurev-matsci-062910-100448.
[5] J. Gonzalez-Julian, S. Onrubia, M. Bram, O. Guillon, Effect of sintering method on the microstructure of pure Cr2AlC MAX phase ceramics, J. Cerma. Soc. Jpn. 124 (4) (2016) 415–420, https://doi.org/10.2109/jcersj2.15263.
[6] J. Gonzalez-Julian, T. Go, D.E. Mack, R. Vaßen, Thermal cycling testing of TBCs on Cr2AlC MAX phase substrates, Surf. Coat. Technol. 340 (2018) 17–24, https://doi.org/10.1016/j.surfcoat.2018.02.035.
[7] M.W. Barsoum, T. El-Raghy, Synthesis and characterization of a remarkable ceramic: Ti3SiC2, J. Am. Ceram. Soc. 79 (7) (1996) 1953–1956, https://doi.org/10.1111/j.1151-2916.1996.tb08018.x.
[8] P. Eklund, M. Beckers, U. Jansson, H. Högberg, L. Hultman, The Mn+1AXn phases: materials science and thin-film processing, Thin Solid Films 518 (8) (2010) 1851–1878, https://doi.org/10.1016/j.tsf.2009.07.184.

[9] N.F. Gao, Y. Miyamoto, D. Zhang, On physical and thermochemical properties of high-purity Ti3SiC2, Mater. Lett. 55 (1–2) (2002) 61–66, https://doi.org/10.1016/S0167-577X(01)00620-6.
[10] H. Wang, T. Webb, J.W. Bitler, study of thermal expansion and thermal conductivity of cemented WC–co composite, Int. J. Refract. Met. Hard Mater. 49 (2015) 170–177, https://doi.org/10.1016/j.ijrmhm.2014.06.009.
[11] A. Petzold, J. Ulbricht, Feuerbeton und betonartige feuerfeste Massen und Materialien. Werkstofftypen, Eigenschaften, Anwendung ; mit 33 Tabellen, Dt. Verl. für Grundstoffindustrie, Leipzig, 1994 (ISBN 3-342-00559-9.).
[12] H.O. Pierson, Handbook of Refractory Carbides and Nitrides. Properties, Characteristics, Processing, and Applications, Noyes Publ, Westwood, NJ, 1996 (ISBN 0-8155-1392-5.).
[13] S. Elomari, M.D. Skibo, A. Sundarrajan, H. Richards, Thermal expansion behavior of particulate metal-matrix composites, Compos. Sci. Technol. 58 (3) (1998) 369–376, https://doi.org/10.1016/S0266-3538(97)00124-3.
[14] R. Arpón, J.M. Molina, R.A. Saravanan, C. García-Cordovilla, E. Louis, J. Narciso, Thermal expansion behaviour of aluminium/SiC composites with bimodal particle distributions, Acta Mater. 51 (11) (2003) 3145–3156, https://doi.org/10.1016/S1359-6454(03)00126-5.
[15] Z. Li, R.C. Bradt, Thermal expansion of the cubic (3C) polytype of SiC, J. Mater. Sci. 21 (12) (1986) 4366–4368, https://doi.org/10.1007/BF01106557.
[16] G.C. Wei, P.F. Becher, Improvements in mechanical properties in SiC by the addition of TiC particles, J. Am. Ceram. Soc. 67 (8) (1984) 571–574, https://doi.org/10.1111/j.1151-2916.1984.tb19174.x.
[17] W. Schedler, Hartmetall für den Praktiker. Aufbau, Herstellung, Eigenschaften und industrielle Anwendung einer modernen Werkstoffgruppe, VDI-Verl, Düsseldorf, 1988 (ISBN 3-18-400803-7.).
[18] L.-H. Tian, C.-X. Li, C.-J. Li, G.-J. Yang, Effect of dispersed TiC content on the microstructure and Thermal expansion behavior of shrouded-plasma-sprayed FeAl/TiC composite coatings, J. Therm. Spray Technol. 21 (3–4) (2012) 689–694, https://doi.org/10.1007/s11666-012-9767-9.
[19] L.H. Ho-Duc, T. El-Raghy, M.W. Barsoum, Synthesis and characterization of 0.3 Vf TiC–Ti3SiC2 and 0.3 Vf SiC–Ti3SiC2 composites, J. Alloys Compd. 350 (1–2) (2003) 303–312, https://doi.org/10.1016/S0925-8388(02)00985-4.
[20] A.Y. Yi, A. Jain, Compression molding of aspherical glass lenses-A combined experimental and numerical analysis, J. Am. Ceram. Soc. 88 (3) (2005) 579–586, https://doi.org/10.1111/j.1551-2916.2005.00137.x.
[21] S. Nollau, A. Kunz, O. Rübenach, G. Pongs, Innovative Optikdesigns durch Präzisionsblankpressen. Anspruchsvolle Optiken und niedrige Kosten müssen kein Widerspruch sein!, Optik & Photonik 6 (1) (2011) 30–34.
[22] H. Kreilkamp, Analyse der Einflüsse auf die Gestaltabweichung gepresster Glasoptiken beim nicht-isothermen Blankpressen, RWTH Aachen Dissertation, 2018. ISBN 978-3-86359-659-0.
[23] H. Dörner, Gläser und Werkzeugwerkstoffe zum Präzisionsblankpressen. Zugl.: Aachen, Techn. Hochsch., Diss., 2010. Ergebnisse aus der Produktionstechnik Prozesstechnologie, Bd. 2011,3, Aachen, Apprimus-Verl, 2011 (ISBN 978-3-86359-013-0).
[24] OHARA GmbH: L-LAH53, Hofheim. https://www.ohara-gmbh.com/fileadmin/user_upload/export-data/pdf/product_datasheets/L-LAH53_Deutsch_.pdf, 2019 last downloaded: 2024.07.18.
[25] C. Racault, F. Langlais, R. Naslain, Solid-state synthesis and characterization of the ternary phase Ti3SiC2, J. Mater. Sci. 29 (13) (1994) 3384–3392, https://doi.org/10.1007/BF00352037.
[26] Y. Zhou, Z. Sun, S. Chen, Y. Zhang, In-situ hot pressing/solid-liquid reaction synthesis of dense titanium silicon carbide bulk ceramics, Mater. Res. Innov. 2 (3) (1998) 142–146, https://doi.org/10.1007/s100190050076.
[27] J.-F. Li, F. Sato, R. Watanabe, Synthesis of Ti3SiC2 polycrystals by hot-isostatic pressing of the elemental powders, J. Mater. Sci. Lett. 18 (19) (1999) 1595–1597, https://doi.org/10.1023/A:1006664416845.
[28] J.-F. Li, W. Pan, F. Sato, R. Watanabe, Mechanical properties of polycrystalline Ti3SiC2 at ambient and elevated temperatures, Acta Mater. 49 (6) (2001) 937–945, https://doi.org/10.1016/S1359-6454(01)00011-8.
[29] Y. Zhang, Y.C. Zhou, Y. Li, Solid–liquid synthesis of Ti3SiC2 particulate by fluctuation procedure, Scr. Mater. 49 (3) (2003) 249–253, https://doi.org/10.1016/S1359-6462(03)00218-5.
[30] A. Feng, T. Orling, Z.A. Munir, Field-activated pressure-assisted combustion synthesis of polycrystalline Ti 3 SiC 2, J. Mater. Res. 14 (3) (1999) 925–939, https://doi.org/10.1557/JMR.1999.0124.
[31] Z. Sun, Z. Zhang, H. Hashimoto, T. Abe, Ternary compound Ti3SiC2: part I. Pulse discharge sintering synthesis, Mater. Trans. 43 (3) (2002) 428–431, https://doi.org/10.2320/matertrans.43.428.
[32] J. Zhu, B. Mei, Fabrication of high-purity Ti3SiC2 by spark plasma sintering (SPS) of elemental powders, J. Mater. Sci. Lett. 22 (12) (2003) 889–890, https://doi.org/10.1023/A:1024418922028.
[33] X. Tong, T. Okano, T. Iseki, T. Yano, Synthesis and high temperature mechanical properties of Ti3SiC2/SiC composite, J. Mater. Sci. 30 (12) (1995) 3087–3090, https://doi.org/10.1007/BF01209221.
[34] S. Yang, Z. Sun, H. Hashimoto, T. Abe, Ti3SiC2 powder synthesis from Ti/Si/TiC powder mixtures, J. Alloys Compd. 358 (1–2) (2003) 168–172, https://doi.org/10.1016/S0925-8388(03)00039-2.
[35] Z.F. Zhang, Z.M. Sun, H. Hashimoto, T. Abe, Effects of sintering temperature and Si content on the purity of Ti3SiC2 synthesized from Ti/Si/TiC powders, J. Alloys Compd. 352 (1–2) (2003) 283–289, https://doi.org/10.1016/S0925-8388(02)01171-4.
[36] M.W. Barsoum, T. El-Raghy, C.J. Rawn, W.D. Porter, H. Wang, E.A. Payzant, C. R. Hubbard, Thermal properties of Ti3SiC2, J. Phys. Chem. Solid 60 (4) (1999) 429–439, https://doi.org/10.1016/S0022-3697(98)00313-8.
[37] T. El-Raghy, M.W. Barsoum, Processing and mechanical properties of Ti3SiC2: I, reaction path and microstructure evolution, J. Am. Ceram. Soc. 82 (10) (1999) 2849–2854, https://doi.org/10.1111/j.1151-2916.1999.tb02166.x.
[38] J.M. Córdoba, M.J. Sayagués, M.D. Alcalá, F.J. Gotor, Synthesis of Ti3SiC2 powders: reaction mechanism, J. Am. Ceram. Soc. 90 (3) (2007) 825–830, https://doi.org/10.1111/j.1551-2916.2007.01501.x.
[39] Z.F. Zhang, Z.M. Sun, H. Hashimoto, Low temperature synthesis of Ti3SiC2 from Ti/SiC/C powders, Mater. Sci. Technol. 20 (10) (2004) 1252–1256, https://doi.org/10.1179/026708304X6103.
[40] D.T. Wan, Y.C. Zhou, Y.W. Bao, In situ reaction synthesis and characterization of Ti3Si(Al)C2/SiC composites, Ceram. Int. 32 (8) (2006) 883–890, https://doi.org/10.1016/j.ceramint.2005.07.004.
[41] R. Radhakrishnan, C.H. Henager, J.L. Brimhall, S.B. Bhaduri, Synthesis of Ti3SiC2/SiC and TiSi2/SiC composites using displacement reactions in the Ti-Si-C system, Scr. Mater. 34 (12) (1996) 1809–1814, https://doi.org/10.1016/1359-6462(95)00663-X.
[42] J. Zhang, L. Wang, W. Jiang, L. Chen, Effect of TiC content on the microstructure and properties of Ti3SiC2–TiC composites in situ fabricated by spark plasma sintering, Mater. Sci. Eng. A 487 (1–2) (2008) 137–143, https://doi.org/10.1016/j.msea.2007.12.004.
[43] W.B. Tian, Z.M. Sun, H. Hashimoto, Y.L. Du, Synthesis, microstructure and mechanical properties of Ti3SiC2–TiC composites pulse discharge sintered from Ti/Si/TiC powder mixture, Mater. Sci. Eng. A 526 (1–2) (2009) 16–21, https://doi.org/10.1016/j.msea.2009.08.029.
[44] B.Y. Islak, E. Ayas, Evaluation of properties of spark plasma sintered Ti3SiC2 and Ti3SiC2/SiC composites, Ceram. Int. 45 (9) (2019) 12297–12306, https://doi.org/10.1016/j.ceramint.2019.03.144.
[45] A. Pourebrahim, H. Baharvandi, H. Foratirad, N. Ehsani, Low temperature synthesis of high-purity Ti3SiC2 via additional Si through spark plasma sintering, J. Alloys Compd. 789 (2019) 313–322, https://doi.org/10.1016/j.jallcom.2019.03.062.
[46] T.L. Ngai, Y. Kuang, Y. Li, Impurity control in pressureless reactive synthesis of pure Ti3SiC2 bulk from elemental powders, Ceram. Int. 38 (1) (2012) 463–469, https://doi.org/10.1016/j.ceramint.2011.07.028.
[47] S. Arunajatesan, A.H. Carim, J. Am. Ceram. Soc. 78 (3) (1995) 667–672, https://doi.org/10.1111/j.1151-2916.1995.tb08230.x.
[48] Z.M. Sun, H. Hashimoto, W. Tian, Y. Zou, Synthesis of the MAX phases by pulse discharge sintering, Int. J. Appl. Ceram. Technol. 7 (6) (2010) 704–718, https://doi.org/10.1111/j.1744-7402.2010.02555.x.
[49] R. German, Sintering Theory and Practice. A Wiley Interscience Publication, Wiley, New York, Chichester, 1996 (ISBN 047105786X.).
[50] Y.S. Touloukian, R.K. Kirby, R.E. Taylor, T.Y.R. Lee, Thermal Expanison. Nonmetallic solids, in: Thermophysical properties of matter. The TPRC data series; a comprehensive compilation of data by the Thermophysical Properties Research Center <TPRC>, Purdue Univ, IFI/Plenum, New York, 1977 (ISBN 0-306-67033-X.).
[51] S. Fries, S. Herzog, D.P. Wilhelm, T. Grunwald, C. Broeckmann, Moulding materials with tailored coefficient of thermal expansion for glass forming, Ceramic forum international 101 (1) (2024) E73–E76, https://doi.org/10.18154/RWTH-2024-02445.
[52] Cornel Fuest: Formgebung von Molybdän- und Titansiliziden über das Pulvermetallformspritzen, Dissertation, Forschungszentrum Jülich, 1994.
[53] H. Sicius, Titangruppe: Elemente der vierten Nebengruppe, in: Handbuch der chemischen Elemente, Springer Spektrum, Berlin, Heidelberg, 2019, pp. 1–47, https://doi.org/10.1007/978-3-662-55944-4_9-2.